Image Segmentation Solutions for Improved Non-Cooperative Target Recognition

ABSTRACT

The number of failed satellites in space is increasing, and they need to be fueled through space docking to extend their life or clean them out of orbit. Visual measurement is widely used in the docking session because of its real-time performance and economy, but the collected images will have background interference, which directly leads to the degradation of the accuracy of visual measurement. Reduce the difficulty of subsequent image processing by solving these problems. For the non-cooperative target of the star-arrow docking ring and the solar sail panel, which are two significant targets, this paper is based on target detection, according to the image difference, binarization, morphological operations and other methods to complete the accurate segmentation of the two targets, which can be more accurately complete the target detection, and the image segmentation effect is obvious. The target image obtained by image segmentation does not contain background interference, which is convenient for feature extraction and matching of the image.

Keywords: visual measurement, non-cooperative targets, target detection, image segmentation

1. INTRODUCTION

With the increasing efforts of mankind's space exploration, the number of artificial satellites in space has also greatly increased, and the number of failed satellites due to malfunction or fuel exhaustion has also increased [1]. Failed satellites not only occupy orbit resources, but also threaten the safety of other satellites [2]. Some of the failed satellites are cooperative satellites, i.e., satellites that can provide cooperative information, in contrast to non-cooperative targets, and visual measurement for non-cooperative targets is a major difficulty [4], which has been studied in various countries [3-5].

Visual measurement is degraded in accuracy and speed because of light, occlusion, background noise and other factors. Visual measurement can get a lot of information about the target, such as size, attitude, etc., through optical imaging, but computers cannot have strong recognition ability and error tolerance space like humans [11-13].Du [14] used the Canny algorithm for edge detection, and used the Hough transform to find a straight line for the rectangular borders of solar sail panels, which in turn determines the rectangle's vertices and edge lengths; He [15] proposed the morphological operations of open and closed operations to extract the edge information of the features, which is significantly improved compared with the traditional methods.

With the development of artificial intelligence, some scholars have introduced machine learning into visual measurement to improve the accuracy and speed of automatically extracting target features, and the existing machine learning methods based on deep neural networks are quite widely used [16-19]. For example, Du [20] designed a keypoint detection network combiningconvolutional neural network(CNN) and Perspective-n-Point (PnP)algorithms, created a non-cooperative target image dataset, trained a BiSeNet-based

model, and performed real-time semantic segmentation of non-cooperative targets, and the satellite recognition accuracy of this method was 99.48%, and the target segmentation accuracy was 98.11%; Wang [21] proposed a new regional Focused Feature Detection (RFD) method to solve this problem and improve target detection accuracy. This method improves the similarity by 10.69%, the extraction rate by 9.04% and the precision by 13.27%.

2. RESEARCH METHODOLOGY

In this study, a non-cooperative target image segmentation method based on target detection is proposed. The method first obtains a convolutional neural network model by creating a training set, then uses the model for target detection of the star-arrow docking ring and the solar sail panel, and finally uses different methods for image segmentation of these two different targets based on the target detection results.

2.1 Target detection

Target detection is the localization and identification of one or more target objects in an image or video. The goal is to detect the location of all targets in an image and assign category labels to each target. Target detection not only determines the presence of a target in an image, but also determines the location of the target in the image. Convolutional neural network based target detection is the commonly used method. The input for target detection is the entire image and the output is the location and category labels of the targets.

2.1.1Dataset creation

The camera in this paper adopts Lt-C4040/Lt-M4040 model CCD (charge coupled device) grayscale camera; the lens in this paper adopts Basler Lens C11-0824-12M-P model lens; according to the requirements of the task to build the satellite model of the equal scale reduction of the pair, as shown in Figure 1.

Figure 1 Satellite model

The satellite model is photographed with the camera, and the distance between the satellite and the camera and the rotation angle need to be changed continuously during the process of photographing. The photographed non-cooperative satellite images are imported into LabelIMG, which is a visualization tool for image calibration,and the target is labeled, which is done by drawing an external rectangular box for the target, and then labeling the target

name corresponding to the rectangular box. For the convenience of name display, this paper simplifies the star-arrow docking ring as 0 and the solar sail panel as 1.

In this paper, a total of 809 images are produced as a dataset for subsequent training and learning of convolutional neural network models.

2.1.2Model training

The dataset produced in the previous section was imported into Yolov5 for model training. The training is based on NVIDIA RTX3090 discrete graphics card, Pytorch version 1.10.0-GPU, and the corresponding CUDA v10.2. The following training parameters are set before the training: the number of training epochs: 700; the training set ratio (train): 0.8, the validation set ratio (val): 0.2; batch-size:16.

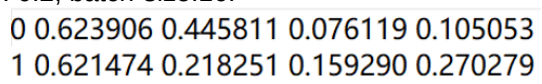

Figure 2 Labeling information

As shown in Fig. 2, Yolov5 can output a txt file of the position size of the box of the detected target, i.e., the label information. Where column 1 represents the target label name, columns 2 and 3 represent the horizontal and vertical coordinates of the box where the target is located in the image, and columns 4 and 5 represent the width and height of the box.

2.2 Image segmentation

In the field of vision, operations such as feature point extraction, feature matching and position estimation need to obtain effective information about the target in the image, but the cluttered background near the target cannot be completely eliminated after Yolov5 detection, and it is necessary to segment the image to obtain a target image free of background interference, so as to facilitate the subsequent image processing to obtain effective information about the target accurately and efficiently.

In this study, two features on the satellite are selected for segmentation, namely the circular target represented by the star-arrow docking ring and the rectangular target represented by the solar sail panel. The image segmentation codes designed in this paper are run on Matlab 2021a.

2.2.1 Circular target segmentation

The star-arrow docking ring always appears independently and the circular feature is relatively easy to recognize because it differs from other features. For circular targets, the shape center of the box can be approximated as the center of the star-arrow docking ring (the center of the circle), as follows:

Step 1 Calculate the center point of the box, i.e., the center of the shape, based on the label information, and set the point as the center of the circle.

Step 2 Calculate the radius of the circle as half of the minimum value of the width and height of the box according to the label information.

Step 3 Draw a circle with the center and radius in steps 1 and 2, keep the original image in the interior of the circle, and create a black mask on the exterior, so that all the pixel gray values are assigned to 0. This can eliminate the need to identify the image features, and quickly get the image of the star-arrow docking exchange.

2.2.2Rectangular target segmentation

Solar sail panels change their attitude continuously during satellite rotation, so the following segmentation method is proposed, taking into account the amount of computation and the possible infinity of the slope of the straight line, among other things:

Step1: Image differencing. According to the label information, the pixels inside the box are kept, and two consecutive frames are differenced to obtain the difference image.

Step 2: Center occlusion. Since the star-arrow docking ring is on the satellite body and the solar sail panels are symmetrically distributed on both sides of the body, the grayscale value of the satellite body part is assigned to 0 with the label information of the star-arrow docking ring.

Step 3: Binarization. The image is binarized using the Otsu method to automatically confirm the threshold value, and the grayscale value of pixels smaller than the threshold value is 0, and vice versa is 255.

Step 4: Connectivity domain analysis. Connectivity domain analysis is performed on the image at this point, i.e., consecutive regions in the image are labeled to get the size of each connectivity domain and other information, the smallest connectivity domains are deleted, and then the remaining connectivity domains are drawn with an external rectangular box.

Step 5: Expansion. Expansion is a morphological operation, the main role in image processing is to expand the boundary points of the object, in short, the expansion operation can make the target larger, can fill the hole in the target.

Step 6: Repeat steps 3 and 4, at this point, the maximum connectivity domain is retained and the outer rectangular box is drawn.

Figure 3 illustrates the rectangular image segmentation process map.

(a) Difference image (b) Center blocked image(c) Binarized image (d) Dilation image

Figure3 Rectangular target segmentation process

3. EXPERIMENTATION AND ANALYSIS

3.1 Target detection experiments

Images were acquired for the satellite model and target detection experiments were performed using a trained convolutional neural network model, with test targets 0 representing the star-arrow docking ring and 1 representing the solar sail panel. The star-arrow docking ring was involved in 130 experiments and the solar sail panel was involved in 160 tests.

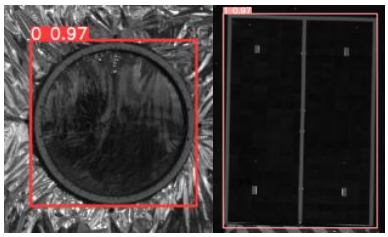

(a) Docking ring detection (b) Solar sail panel detection

Figure4 Rectangular target segmentation process

As can be seen from Fig. 4, the target detection effect is very stable, which can ensure the detection success rate at about 97%, and can also determine the box of the target location.

Table 1 Target detection experimental data

test objective	0	1
Number of tests N	130	160
Number of successes Ne	126	151

The confidence level for this paper is calculated as.

$$S = Ne/N \tag{3.1}$$

According to Table 1, The confidence level for target detection can be determined by calculating the average confidence levels individually for the star-arrow docking ring (96.92%) and the solar sail panel (94.37%). The combined average confidence level for both targets is then computed as 95.51%. It can be seen that the circular target achieves a very high detection confidence due to its high degree of rotational invariance, and the rectangular target is detected with a slightly lower effect, but also with more than 94% confidence. This experiment verifies the completeness of the dataset produced in this paper, as well as the reliability of the convolutional neural network model.

Successfully detected targets, Yolov5 are outputting the labeling information corresponding to the target.

3.2 Image segmentation experiment

Based on the labeling information of target detection in the previous section, image segmentation experiments are conducted for circular and rectangular targets using the corresponding methods.

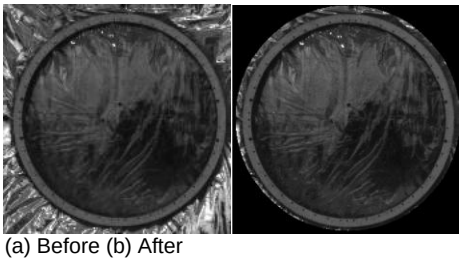

(a) Before (b) After

Figure5Circular target segmentation before and after

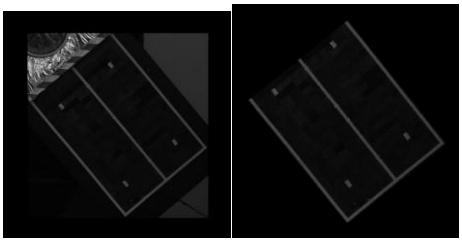

(a) Before (b) After

Figure6Rectangular target segmentation before and after

Based on the method proposed in this paper, the image segmentation of the star-arrow docking ring and the solar sail panel can be realized, and from the segmentation comparison results in Fig. 5 and Fig. 6, the effect of image segmentation is very obvious, especially the cluttered background on the outside of the solar sail panel are completely eliminated, and only the information on the sail panel is retained.

As shown in Fig. 7, in the traditional method, image segmentation using only the image difference is very ineffective and cannot completely remove the background information from the edges of solar sail panels. The method in this paper can achieve 100% success rate of image segmentation based on the target detection results.

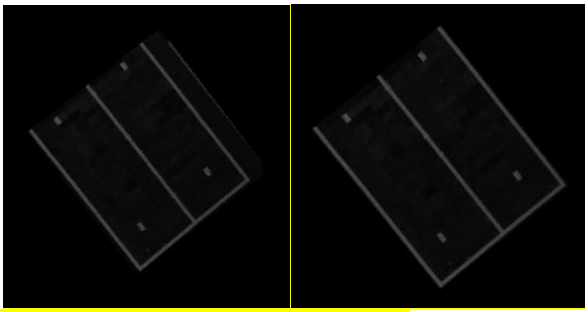

(a)Traditional method(b) Methods in this paper

Figure7A comparison betweentraditional method with the method in this paper

The computational time required by the algorithm in the literature[15] using a combination of open and closed operations is about 0.19 seconds, and the algorithm in this paper takes 0.16 seconds, which saves 15.29% of the time in the morphological processing step. Experiments verify the feasibility of the segmentation method in this paper, and from the results, the method in this paper has very high accuracy and efficiency, and fully realizes the fully automatic image segmentation task without human intervention.

4. CONCLUSION

Various countries are accelerating the process of space exploration, and image misrecognition due to the influence of the complex background in space is a major problem in the development of space industry. In this study, a non-cooperative satellite image segmentation method based on Yolo target detection is proposed, which successfully reduces the interference of the background on the target, reduces the difficulty of the subsequent image processing, feature extraction, etc. It provides a solution idea for other scholars, and has a positive significance in promoting the visual measurement of non-cooperative satellites.

COMPETING INTERESTS

Authors have declared that no competing interests exist.

AUTHORS' CONTRIBUTIONS

This work was carried out in collaboration among all authors. All authors read and approved the final manuscript.

REFERENCES

1. Thienel J K, Sanner R M. Hubble space telescope angular velocity estimation during th e robotic servicing mission[J]. Journal of guidance, control, and dynamics, 2007, 30(1): 29-34.

2. Miravet C, Pascual L, Krouch E, et al. An image-based sensor system for autonomous r endez-vous with uncooperative satellites[J]. arXiv preprint arXiv:0807.4478, 2008.

3. Li W J, Cheng D Y, Liu X G, et al. On-orbit service (OOS) of spacecraft: A review of eng ineering developments[J]. Progress in Aerospace Sciences, 2019, 108: 32-120.

4. Hammer M, Hebel M, Borgmann B, et al. Potential of lidar sensors for the detection of UAVs[C]//Laser Radar Technology and Applications XXIII. SPIE, 2018, 10636: 39-45.

5. Ding M, Zhang Z, Jiang X, et al. Vision-Based Distance Measurement in Advanced Driving Assistance Systems[J]. Applied Sciences, 2020, 10(20): 7276.

6. Zhe T, Huang L, Wu Q, et al. Inter-vehicle distance estimation method based on monocular vision using 3D detection[J]. IEEE transactions on vehicular technology, 2020, 69 (5): 4907-4919.

7. Zhu Z, Xiang W, Huo J, et al. Non-cooperative target pose estimation based on improved iterative closest point algorithm[J]. Journal of Systems Engineering and Electronics, 2022, 33(1): 1-10.

8. Zhang L, Wu D M, Ren Y. Pose measurement for non-cooperative target based on visual information[J]. IEEE Access, 2019, 7: 106179-106194.

9. Han S, Niu P, Luo S, et al. A Novel Deep Convolutional Neural Network Combining Global Feature Extraction and Detailed Feature Extraction for Bearing Compound Fault Diagnosis[J]. Sensors, 2023, 23(19): 8060.

10. Du X, Liang B, Xu W, et al. Pose measurement of large non-cooperative satellite based on collaborative cameras[J]. Acta Astronautica, 2011, 68(11-12): 2047-2065.

11. He Y B, Zeng Y J, Chen H X, et al. Research on improved edge extraction algorithm of rectangular piece[J]. International Journal of Modern Physics C, 2018, 29(01): 1850007.

12. He Q, Xu A, Ye Z, et al. Object detection based on lightweight YOLOX for autonomous driving[J]. Sensors, 2023, 23(17): 7596.

13. Taigman Y , Yang M , Ranzato M ,et al.DeepFace: Closing the Gap to Human-Level Performance in Face Verification[C]//IEEE Conference on Computer Vision & Pattern Recognition.IEEE Computer Society, 2014.DOI:10.1109/CVPR.2014.220.

14. Sallab A , Abdou M , Perot E ,et al.Deep Reinforcement Learning framework for Autonomous Driving[J].Electronic Imaging, 2017, 2017(19):70-76.DOI:10.2352/ISSN.2470-1173.2017.19.AVM-023.

15. Esteva, Andre; Robicquet, Alexandre; Ramsundar, Bharath; Kuleshov, Volodymyr; DePristo, Mark; Chou, Katherine; Cui, Claire; Corrado, Greg; Thrun, Sebastian; Dean, Jeff (2019). A guide to deep learning in healthcare. Nature Medicine, 25(1), 24–29. doi:10.1038/s41591-018-0316-z

16. Du H, Hu H, Wang D, et al. Autonomous measurement and semantic segmentation of non-cooperative targets with deep convolutional neural networks[J]. Journal of Ambient Intelligence and Humanized Computing, 2023, 14(6): 6959-6973.

17. Wang J, Alshahir A, Abbas G, et al. A Deep Recurrent Learning-Based Region-Focused Feature Detection for Enhanced Target Detection in Multi-Object Media[J]. Sensors, 2023, 23(17): 7556.